COHERENT DIFFRACTION RADIATION AS A TOOL FOR LONGITUDINAL BEAM PROFILE DIAGNOSTICS AT CTF3*

K. Lekomtsev#, G. Blair, G. Boorman, P. Karataev, M. Micheler, John Adams, Institute at Royal Holloway, University of London, Egham, UK
R. Corsini, T. Lefevre, CERN, Geneva, Switzerland

Abstract

A setup for the investigation of Coherent Diffraction Radiation from targets with various configurations as a tool for non-invasive longitudinal electron beam profile diagnostics has been designed and installed in the CRM line of the CLIC Test Facility 3(CTF3 at CERN) [1]. In this report we present the status of the experiment. Recently we have upgraded the system by installing the second target to suppress synchrotron radiation background. In this report we shall also demonstrate the results on simulations of CDR spatial distribution from a two target configuration.

INTRODUCTION

A novel scheme for a drive beam generation has been proposed for the future Compact Linear Collider (CLIC), in which a long bunch train with low bunch repetition frequency will be accelerated with low RF frequency. Subsequent packets of this bunch train are interleaved in isochronous rings thereby increasing the bunch repetition frequency and shortening the bunch train with a corresponding increase in peak current. The main goals of CTF3 are to test new RF power generation scheme and to produce 12 GHz RF power at the nominal peak power and pulse length, such that all 12 GHz components for CLIC can be tested at nominal parameters [2]. The optimization and monitoring of the longitudinal charge distribution in a bunch is crucial for the maximization of luminosity and for an optimal performance of the CLIC drive beam.

Diffraction radiation (DR) is widely used as a tool for transverse [3] and longitudinal [4] beam parameter monitoring. DR arises when a charged beam passes by in the vicinity of a target, the effect of the beam interaction with the target material is minimal and a smaller perturbation to the beam is produced compared with other diagnostics, such as transition radiation. Coherent Diffraction Radiation (CDR) was suggested as a mechanism for the coherent radiation generation due to its non-invasive nature and is utilised in this experiment. The intensity of CDR is proportional to the square of the beam current and it produces much higher power than that of incoherent radiation. A spectral distribution of CDR contains information about the distribution of electrons in the bunch.

*Work supported by the EU under contract PITN-GA-2008-215080.
#K.V.Lekomtsev@rhul.ac.uk

SIMULATIONS

In this chapter the current progress on simulations of CDR from two targets will be reported. The schematic layout of the two target configuration is shown in Fig.1.

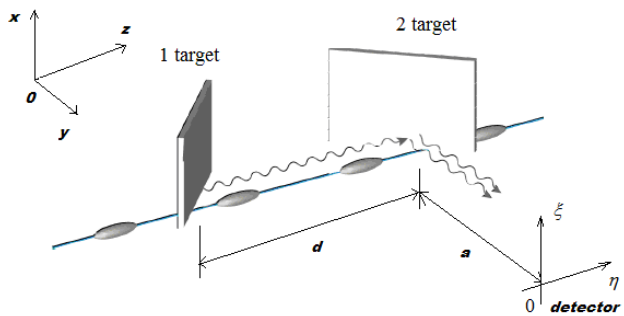

Figure 1: Schematic layout of the targets configuration.

Backward Diffraction Radiation from the Second Target

For calculations we shall use a classical theory of Diffraction Radiation (DR), based on Huygens principle of plane wave diffraction. In reality classical DR theory describes backward DR only. However for a metallic foil and millimetre wavelengths we can use an ideal conductor approximation. In this case BDR characteristics coincide with FDR ones [5]. A particle field is introduced as a superposition of its pseudo-photons and when they are scattered off a target surface they are converted into real ones and propagate either in the direction of specular reflection (BDR) or along the particle trajectory (FDR).

Let an electron move along the z-axis. Each point of the target surface can be represented as an elementary source. Two polarization components of DR can be represented as a superposition of the waves from all elementary sources at a distance **r** from the target [5]:

$$E_{x,y} = \frac{1}{4\pi^2}\iint E^i_{x,y}\left(x_r, y_r\right)\frac{e^{i\varphi}}{r}dy_r dx_r. \qquad (1.1)$$

In (1.1) $x_r = \rho_r \sin\psi_r$ and $y_r = \rho_r \cos\psi_r$ are the coordinates of the particle field, ρ_r and ψ_r are the radius and azimuthal angle of the particle pseudo photon field in polar coordinate system; $E^i_{x,y}$ gives an amplitude of an arbitrary elementary source positioned at x_r and y_r on the target surface; φ defines the phase advance of the

photons emitted by each elementary source at x_r and y_r to an observation point; r is the distance from the arbitrary elementary source on the target to the observation plane.

DR from the second target can be written as:

$$E^2_{x,y} = \frac{1}{4\pi^2}\frac{iek}{\pi\gamma}\frac{e^{ika}}{a}\iint\begin{pmatrix}\frac{x_2}{\sqrt{x_2^2+y_2^2}}\\ \frac{y_2}{\sqrt{x_2^2+y_2^2}}\end{pmatrix}K_1\left(\frac{k}{\gamma}\sqrt{x_2^2+y_2^2}\right)\times \exp\left[\frac{ik}{2a}\left((x_2-\xi)^2+(y_2-\eta)^2\right)\right]dx_2dy_2, \quad (1.2)$$

where x_2 and y_2 are the coordinates at the second target surface, ξ and η are the coordinates at the observation plane, a is the distance between the second target and the observation plane and k is the wave number.

CDR spatial distribution in general form can be calculated as:

$$\frac{d^2W^{DR}}{d\omega d\Omega} = 4\pi^2k^2a^2\left[\left|E_x^{DR}\right|^2+\left|E_y^{DR}\right|^2\right]. \quad (1.3)$$

Forward Diffraction Radiation from the First Target

Assuming that for our wavelength and a metallic foil FDR and BDR are identical we obtain FDR from the first target which propagates towards the second target and is diffracted from it. The first stage of the process is electric field of FDR produced from the first target on the surface of the second one and the second stage is reflection from the second target, which gives us final result:

$$E^{1\to2\to obs.plane}_{x,y} = E^1_{x,y} = \frac{1}{4\pi^2}\frac{iek}{\pi\gamma}\frac{e^{ikd}}{d}\frac{e^{ika}}{a}\iint_{x_2,y_2}\iint_{x_1,y_1}\begin{pmatrix}\frac{x_1}{\sqrt{x_1^2+y_1^2}}\\ \frac{y_1}{\sqrt{x_1^2+y_1^2}}\end{pmatrix}\times K_1\left(\frac{k}{\gamma}\sqrt{x_1^2+y_1^2}\right)\exp\left[\frac{i\pi}{\lambda d}(x_1-x_2)^2+\frac{i\pi}{\lambda a}(x_2-\xi)^2\right]\times \exp\left[\frac{i\pi}{\lambda d}(y_1-y_2)^2+\frac{i\pi}{\lambda a}(y_2-\eta)^2\right]dx_1dy_1dx_2dy_2. \quad (2.1)$$

where x_1 and y_1 are the coordinates at the first target surface and d is the distance between the targets.

Coherent Diffraction Radiation from two targets

Once two radiation components are obtained we are able to derive CDR distribution from two targets. As we observe interference between BDR from the second target and FDR from the first target the following formula for the radiation spatial distribution is applied:

$$\frac{d^2W^{CDR}_{x,y}}{d\omega d\Omega} = 4\pi^2k^2a^2\left[\left(\mathrm{Re}\,E^1_{x,y}-\mathrm{Re}\left[E^2_{x,y}\exp\left(-\frac{ikd}{\beta}\right)\right]\right)^2+\left(\mathrm{Im}\,E^1_{x,y}-\mathrm{Im}\left[E^2_{x,y}\exp\left(-\frac{ikd}{\beta}\right)\right]\right)^2\right], \quad (3.1)$$

where $E^1_{x,y}$ and $E^2_{x,y}$ are FDR from the first target and BDR from the second target calculated in the previous subsections, $\beta = v/c$ is the speed of an electric charge in terms of the speed of light. Term $\exp(-ikd/\beta)$ defines the phase delay due to the particle moving from the first target to the second one.

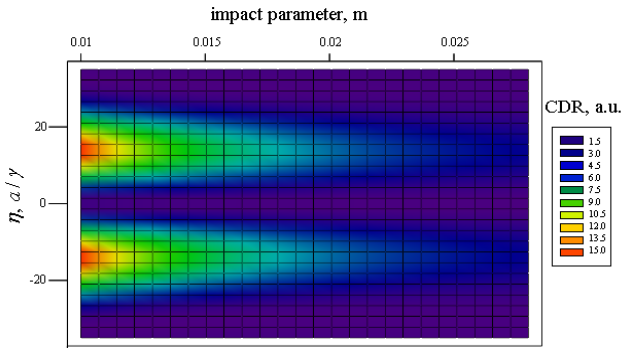

Figure 2: Calculated CDR distribution (horizontal polarization), when the first target is out.

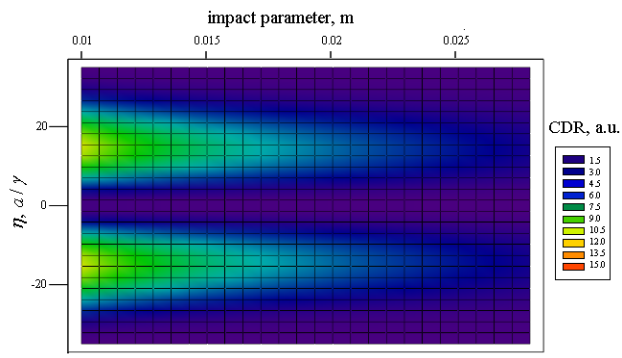

Figure 3: Calculated CDR distribution (horizontal polarization), when the first target is in.

In Fig. 2 and 3 CDR distributions were calculated for the following parameters: the targets dimensions $40\times60mm$, the electron beam energy $\gamma = 235$, the impact parameters $h_{1t\,\mathrm{arg}} = h_{2t\,\mathrm{arg}} = 10mm$ i.e. (when all targets are in) and $h_{1t\,\mathrm{arg}} = 30mm; h_{2t\,\mathrm{arg}} = 10mm$ i.e. (when the first target is out), the wavelength is $\lambda = 5mm$, the observation plane is at $a = 2m$, the distance between the targets is $d = 0.25m$.

In Fig. 3 the effect of destructive interference can be seen with relative decrease of the intensity by approximately 30 percent, compared to the distribution in Fig. 2.

EXPERIMENTAL RESULTS

CDR Distribution Scans

2D scans over the second target orientation and translation of horizontal CDR polarization component, were performed for SBD detector DXP15 (50-75GHz) and shown in Fig. 4 and 5.

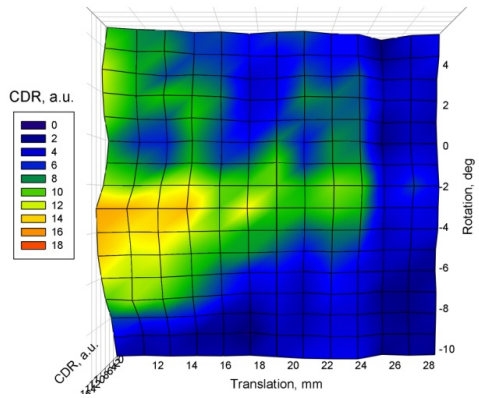

Figure 4: Measured CDR distribution when the first target is out and $h_{1t\arg} = 30mm; h_{2t\arg} = 10mm$.

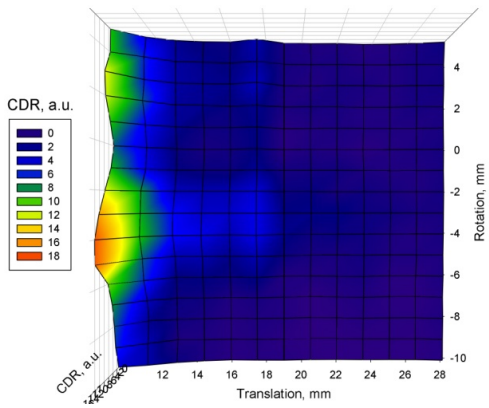

Figure 5: Measured CDR distribution when both targets are in and the impact parameters are $h_{1t\arg} = h_{2t\arg} = 10mm$.

Presented distributions agree fairly well with the calculated CDR distributions, however distortions are observed which might be caused by backgrounds from the CRM line beam dump and remaining part of the Synchrotron Radiation background. We observe strong backgrounds suppression in Fig. 5 compared to the distribution in Fig. 4, which proves the effectiveness of the two target configuration for blocking backgrounds originating from upstream the setup. Inequality of peak intensities is the fact which needs to be analyzed more thoroughly.

Interferometric Measurements

To reconstruct the longitudinal electron beam profile at CTF3 the CDR spectrum has to be measured. It contains information about the longitudinal electron distribution:

$$S(\omega) = \left[N_e + N_e(N_e - 1)F(\omega)\right]S_e(\omega) \qquad (4.1)$$

$S(\omega)$ is the signal from the detector. A Michelson interferometer is installed to measure $S(\omega)$. In the interferometer a new broadband pyroelectric detector with broad wavelength response from x-ray to far infrared spectrum with a specially coated 1mm – diameter sensitive element was used. Due to the very small sensitive element in the detector, a Polished Tsurupica Focusing lens (diameter 50.8 mm, focal length 50mm) was installed in front of the pyroelectric detector in order to increase the performance of the setup.

$S_e(\omega)$ is the single electron radiation spectrum, which can be derived by integrating the simulated radiation distribution obtained at the observation plane (ξ,η) over the detector aperture.

N_e can be measured by means of OTR measurements setup installed further down at the CRM line.

Consequently the longitudinal bunch profile can be calculated from experimentally obtained form factor using a Kramers-Kronig relation [6].

CONCLUSIONS AND OUTLOOK

Background contribution studies have been performed. 2D scans of radiation distribution have been done to prove that the second target is effectively blocking the backgrounds originating from upstream the setup. Measurements have been performed for CDR and different target positions were tested in order to find the optimal two target configuration. The experimental results were compared to the simulations and good agreement was revealed, apart from the inequality of peak intensities and distortions caused by backgrounds.

Interferometric measurements have not been finalized due to insufficient sensitivity of the pyroelectric detector and also tough background conditions. As a solution a new, more sensitive pyroelectric detector will be installed and setup shielding will be improved in the near future.

REFERENCES

[1] M. Micheler et al., Proc. IPAC, Kyoto, Japan (2010).
[2] G. Geschonke et al., CTF3 Design report, CERN /PS 2002-08 (2002).
[3] P. Karataev et al., Phys. Rev. Lett. 93 (2004) 244802.
[4] M. Castellano et al., Phys. Rev. E 63 (2001) 056501.
[5] M.L Ter-Mikaelyan, High Energy Electromagnetic Processes in Condensed Media, Wiley-Interscience, New York (1972).
[6] M. Micheler et al., Proc. RREPS-09, Zvenigorod, Russia (2010).